Transfer coupling or neck formation effects on sub-barrier fusion

J. M. B. Shorto,[1] P. R. S. Gomes,[1] J. Lubian,[1] L. F. Canto,[2] and P. Lotti[3]

[1]*Instituto de Física, Universidade Federal Fluminense, Avenida Litoranea s/n, Gragoatá, Niterói, Rio de Janeiro 24210-340, Brazil*

[2]*Instituto de Física, Universidade Federal do Rio de Janeiro, Caixa Postal 68528, Rio de Janeiro 21941-972, Brazil*

[3]*Istituto Nazionale di Fisica Nucleare, Sezione di Padova, Via F. Marzolo 8, I-35131 Padova, Italy*

(Received 10 February 2010; revised manuscript received 2 March 2010; published 1 April 2010)

The role of transfer channels or neck formation in sub-barrier fusion is investigated by using a reliable double-folding potential as the bare potential and a new method, recently developed, that allows the disentangling of transfer-channel effects on the fusion cross section.

DOI: 10.1103/PhysRevC.81.044601 PACS number(s): 25.60.Pj, 25.60.Gc, 24.10.Eq

I. INTRODUCTION

Sub-barrier fusion was a widely investigated subject in past decades. Among several tens of papers on this subject, we give as examples some comprehensive reviews [1–5]. Nowadays, it is well established that couplings with low-lying collective excitations lead to strong enhancements of the fusion in this energy range. However, the effects of the other couplings or degrees of freedom, such as nucleon or cluster transfer channels and the breakup of weakly bound nuclei, are not yet fully understood and are currently under investigation. One of the reasons why the coupling of the transfer channels is not yet fully understood is the lack of exclusive transfer data that would allow the determination of suitable spectroscopic factors to be used in the coupled-channel (CC) calculations. An alternative approach to handle the global effect of several transfer channels on sub-barrier fusion is to use the concept of a gross feature of nuclear matter, that is, the formation of a neck between two liquid drops representing the collision partners [6]. So, the neck degree of freedom accounts for the average contribution from the couplings to the several open transfer channels. Nevertheless, it also represents the influence of closed transfer channels and processes like the orbiting of nucleons or clusters around the colliding nuclei, as quasimolecular states. In the neck formation model [6,7], the fusion cross section is expressed in terms of tunneling probabilities through the two-dimensional (radial and neck coordinates) barrier. The enhancement of the fusion cross section is then determined through a comparison of cross sections at energies far below the Coulomb barrier. The above-described cross section is compared with that obtained by the one-dimensional barrier penetration model (radial coordinate only). The two cross sections are plotted on a logarithmic scale and the enhancement is measured by the shift, ΔE, needed for the low-energy tail of the one-dimensional tunneling cross section to agree with the two-dimensional one. This shift is attributed to the sum of two effects: the first is related to the bulk properties of nuclear matter and can be approximately described by the neck formation model, whereas the second corresponds to the nuclear structure characteristics of the colliding nuclei such as their static deformations or surface vibrations. Making a similar comparison between the experimental and the one-dimensional cross sections, one determines the experimental shift, $\Delta E_{\rm exp}$. The difference between these two energy shifts, $\Delta E_{\rm exp}$ and ΔE, should be attributed to the couplings with the channels, which depend on the details of the nuclear structure [7]. Such effects cannot be handled by liquid drop treatments.

In the present work, we investigate the inclusive influence of the transfer channels on the sub-barrier fusion cross section using a recently developed method to analyze fusion data [8]. This method consists of reducing the fusion data according to a prescription through which all channel coupling effects that can be accounted for are eliminated from the cross section. If there are no other relevant channels, the reduced cross section coincides with a benchmark cross section, which is called the *universal fusion function* (UFF). Otherwise, the difference can be traced back to the influence of the channels that were left out of the CC calculation. This reduction method has been successfully applied to several collisions of weakly bound nuclei [8,9]. In these cases, the focus of the investigation was the influence of the breakup channel on fusion. Here we apply this method to strongly bound channels, where the breakup couplings are not relevant. We investigate the influence of the transfer channels on fusion.

The paper is organized as follows. In Sec. II, a brief description is given of the double-folding potential used in the calculations. In Sec. III, the fusion function method to reduce fusion data is reviewed. In Sec. IV, the fusion function method is used to investigate the influence of transfer on fusion, considering some reactions. Finally, in Sec. V, the conclusions of the present work are summarized. The reactions chosen to be analyzed in the present paper are the ones that showed anomalous large values of the experimental energy shift $\Delta E_{\rm exp}$ in a previous systematic investigation of neck formation effects on the sub-barrier fusion [7]. In addition, we study the ^{132}Sn + ^{64}Ni reaction, where the projectile is a radioactive neutron-rich nucleus with different characteristics from the also radioactive neutron- and proton-rich ^{6}He and ^{17}F nuclei already studied in Ref. [8].

II. THE DOUBLE-FOLDING POTENTIAL USED

Fusion cross sections for different reactions differ in three ways. First, differences arise from the system sizes and charges, leading to different Coulomb barrier heights, radii, and curvatures. The second difference is in the details of the optical potential, which are also affected by the binding energies of the valence nucleons and other effects such as

neutron-to-proton ratio. We refer to the differences arising from all these reasons as *static effects*. Finally, the third difference involves the effects of the couplings with various low-lying excited channels, transfer channels, or breakup. We call them *dynamic effects*.

As a first step for the investigation of the sub-barrier fusion problem, one should compare the data with reliable theoretical predictions. A well-established fact is the strong dependence of the theoretical calculations on the choice of the interaction potential to describe nuclear reactions. So, the choice of an appropriate nuclear bare interaction between two colliding nuclei is a crucial step in the data interpretation. In the late 1970s, several phenomenological interaction potentials were proposed for heavy-ion collisions. Among them we cite, as examples, Refs. [10–14]. Barrier parameters were extracted with some parametrization, and the fusion cross sections above the barrier could be well reproduced, but not the sub-barrier fusion. After that, several improvements were made in the potentials, including the search of other degrees of freedom, to explain fusion at the sub-barrier energy regime. In particular, the original proximity potential proposed by Blocki *et al.* [11] was subjected to improvements that give special attention to the curvature of the potential. Important works were published by Puri and collaborators [15–19], in which the potential dependence on the isospin was proposed and investigated for several neutron-rich and neutron-deficient colliding nuclei within the framework of the Skyrme energy model. They show that the change in the neutron number modifies the barrier height, position, and diffuseness. By using large surface corrections, the sub-barrier fusion of several systems could be successfully explained. Other works on modified proximity potentials also considered the radius isospin dependent [20,21] and showed very good results.

An alternative natural choice in the determination of a reliable bare potential is to use a double-folding potential based on a system of realistic densities or the use of experimental densities, when available. In the present work we use the São Paulo potential (SPP) [22,23]. This potential is based on a double-folding potential and on the Pauli nonlocality involving the exchange of nucleons between projectile and target, and it is strongly supported by experimental evidence. As for the effective nucleon-nucleon interaction, it is the most widely used realistic interaction, M3Y [24,25], with two possible versions, Reid and Paris. Within this model, the nuclear interaction is connected with the folding potential V_F through the expression $V_N(R) = V_F(R)\exp(-4v^2/c^2)$, where c is the speed of light and v is the local relative velocity between the two nuclei. With the aim of providing a parameter-free description of the nuclear interaction, the SPP model includes an extensive systematic of nuclear densities [23,26]. The two-parameter Fermi (2pF) distribution is assumed to be a good approximation to describe the densities. The radii of the 2pF distributions are well represented by $R_0 = 1.31A^{\frac{1}{3}} - 0.84$ fm, where A is the number of nucleons of the nucleus. The values obtained for the diffuseness of the matter distributions are similar throughout the periodic table and present small variations around the average value $a = 0.56$ fm. Within the context of this realistic systematic, the SPP does not contain any adjustable parameter. Therefore, this model is a powerful tool to make predictions for quite different reactions and energies. For bombarding energies around the Coulomb barrier, the energy-dependent term of the SPP can be ignored because the relative velocity between the interacting nuclei is close to zero in this energy regime, and the SPP becomes, basically, a double-folding potential. The SPP was successfully used to describe several reaction mechanisms for a large number of systems in a wide energy range, without any parameter fit procedure [27–29], including fusion excitation functions and barrier distributions for weakly bound nuclei [30,31] and the fusion of halo nuclei [32]. When the SPP is used in the analysis of elastic scattering, an imaginary part is included [33–36]. This imaginary potential has the same form as the real part and only one free parameter, its strength. In such a situation using a realistic potential, the static effects are taken into account and the difference between the fusion data and the theoretical predictions are due to the coupling effects. The results of the SPP predictions are shown in Fig. 1 for the barrier of the reaction of ^{6}He + ^{238}U by considering ^{6}He as a "normal-density" nucleus and with its actual density corresponding to a halo nucleus. One can observe that the halo characteristics lead to a lower and thicker barrier.

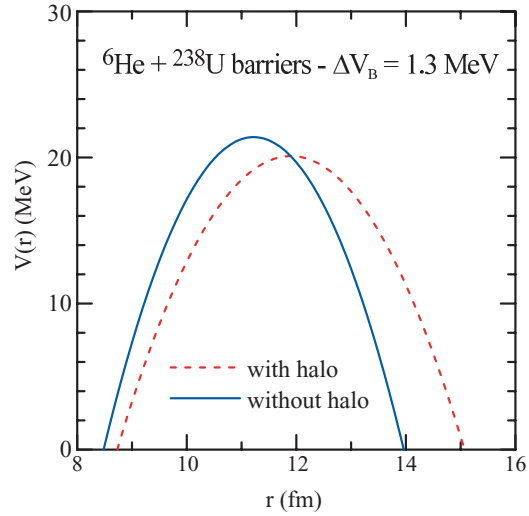

FIG. 1. (Color online) Coulomb barriers for the reaction ^{6}He + ^{238}U predicted by SPP considering two situations: ^{6}He with a "normal density" (solid curve) and with its actual density, taking into account its halo structure (dashed curve).

III. REDUCTION OF THE FUSION DATA

The comparison of data with theoretical predictions is restricted to a single reaction. Because direct comparisons of data for different reactions are not allowed, it is not convenient for a systematic study of the sub-barrier fusion problem for several systems. A direct comparison of different reactions would be distorted by differences such as the projectile's charge or size. It is then necessary to reduce the data in a way that the influence of such factors would be washed

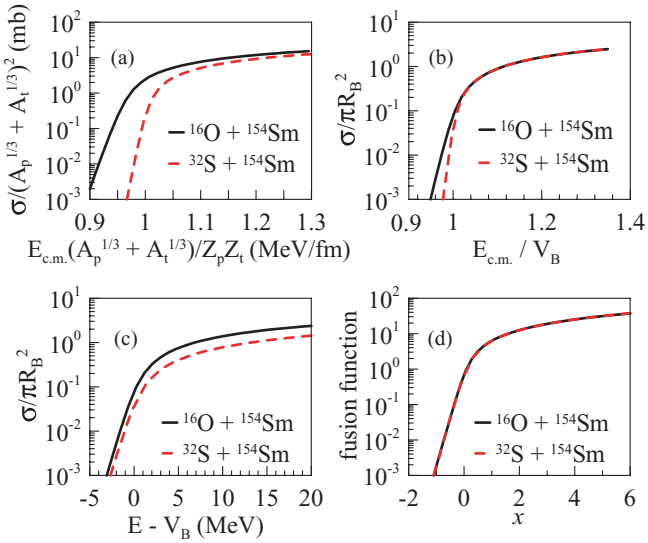

FIG. 2. (Color online) Different procedures to reduce fusion cross sections for the interaction of ^{16}O, ^{32}S + ^{154}Sm. See text for details.

out. For this purpose, different proposals can be found in the literature. A few years ago, a method was proposed [37] that should show both static and dynamic effects simultaneously. However, if one wants to eliminate the static effects, the renormalization procedure should be performed with the use of realistic values of V_B, R_B, and $\hbar\omega$, height, radius, and curvature of the Coulomb barrier [6,7], respectively. Figure 2(a) shows the reduction proposed by Gomes [37] for two reactions. Figures 2(b) and 2(c) show two of the most widely used reduction procedures for the same reactions. The curves are predictions from the optical model calculations using the bare SPP. If the reduction procedures were able to eliminate static effects, both curves would be similar. One can notice that the three procedures fail. Recently [8], aiming to obtain a systematic investigation of the fusion of weakly bound systems, we proposed a reduction procedure that eliminates all static effects from the fusion cross section. It consists of transforming the collision energy and the fusion cross section to the dimensionless quantities

$$E \rightarrow x = \frac{E - V_B}{\hbar\omega}, \quad \sigma_F \rightarrow F(x) = \frac{2E}{\hbar\omega R_B^2}\,\sigma_F. \qquad (1)$$

The barrier parameters are extracted from the optical potential used, which in our work is the SPP. Other potentials can be used. $F(x)$ is called fusion function.

One can determine the fusion function, $F(x)$, using the cross section σ_F in Eq. (1) predicted by the optical model calculation. This fusion function is system independent when σ_F is accurately described by Wong's formula [38]. In this case $F(x)$ becomes

$$F(x) \rightarrow F_0(x) = \ln[1 + \exp(2\pi x)]. \qquad (2)$$

Note that $F_0(x)$ depends exclusively on the dimensionless variable x; it is the same function for any fusion reaction. For this reason it is called the universal fusion function (UFF). It was shown in Ref. [8] that Wong's formula gives a very good description of the fusion cross section of the optical model at near-barrier energies for reactions with $Z_P Z_T \gtrsim 500$. The first step to use this method to analyze fusion data is to build the experimental fusion function, $F_{\rm exp}(x)$. This is performed by using the experimental fusion cross section in Eq. (1). The result is then compared with $F_0(x)$, which is used as a benchmark. For realistic choices of the optical potential in the study of reactions where channel couplings do not have a strong influence on the fusion, one expects that $F_{\rm exp}(x) \simeq F_0(x)$.

However, in most cases the fusion cross section is strongly affected by channel couplings. To extend the use of the method to the analysis of fusion data of such reactions, one introduces the renormalized experimental fusion function,

$$\bar{F}_{\rm exp}(x) = \frac{F_{\rm exp}(x)}{\mathcal{R}(x)}, \quad \text{with} \quad \mathcal{R}(x) = \frac{\sigma_F^{\rm CC}}{\sigma_F}, \qquad (3)$$

where σ_F is the theoretical cross section with all couplings switched off, and $\sigma_F^{\rm CC}$ is the cross section obtained from a CC calculation including a set of channels, $\mathcal{A}$. When all relevant channels are included in $\mathcal{A}$ and the correct coupling strengths are used, $\bar{F}_{\rm exp}(x)$ should match our benchmark. If, however, some relevant set of channels, $\mathcal{B}$, is left out of the CC calculation, there is no agreement. In this case, the difference between the two fusion functions measures the effects of those channels left out of the calculation.

This reduction procedure was also submitted to the test of Fig. 2. The results are shown in Fig. 2(d). One can observe that the curves for the two reactions cannot be distinguished, which indicates that the influence of the potential barrier and the system's mass was fully eliminated.

In previous works [8,9], when the present reduction method was used to investigate the effect of the coupling of breakup-plus-transfer channels on the fusion of weakly bound nuclei, the set of channels, $\mathcal{A}$, included the inelastic excitations of bound states and the set $\mathcal{B}$ was the breakup-plus-transfer channels. In the present work we apply this method in tightly bound systems, for which large sub-barrier fusion enhancement was previously observed and the existence of neck formation was suggested [6,7]. We also investigate recent data using a radioactive neutron-rich projectile [39,40]. The set $\mathcal{A}$ is the same as before (i.e., the inelastic excitations of bound states). Set $\mathcal{B}$ includes the transfer channels. As a bare potential, we use the SPP in all calculations.

IV. ASSESSING THE INFLUENCE OF TRANSFER CHANNELS ON FUSION

A. Collisions of ^{154}Sm with different projectiles

The ^{154}Sm nucleus is known to have a very large permanent deformation. Therefore, the sub-barrier fusion cross sections in collisions of heavy-ion beams with ^{154}Sm targets are expected to be strongly enhanced by the couplings with rotational channels. This point is illustrated in Fig. 3, where we show fusion cross sections for four reactions: ^{16}O + ^{154}Sm [41], ^{28}Si + ^{154}Sm [42], ^{32}S + ^{154}Sm [43], and ^{48}Ca + ^{154}Sm [44,45]. The CC calculations represented by solid lines were performed using the FRESCO code [46]. The calculations

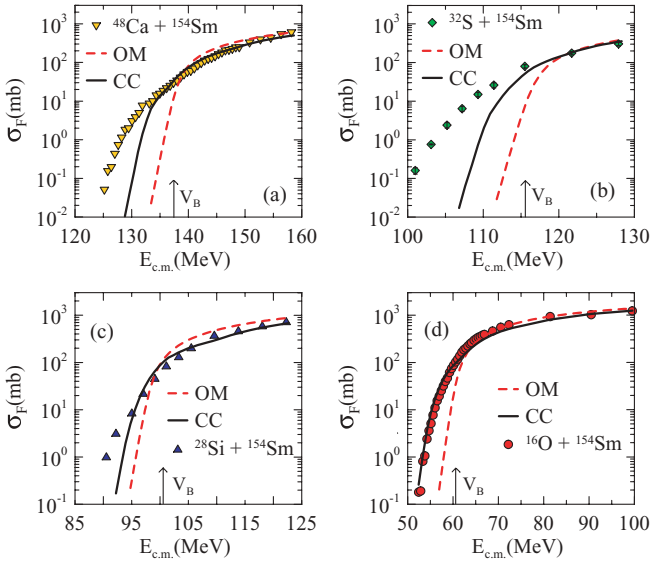

FIG. 3. (Color online) Fusion cross sections in collisions of several projectiles with ^{154}Sm targets. The dashed (OM) and solid (CC) lines correspond, respectively, to predictions of optical model and coupled-channel calculations. In each case, the position of the Coulomb barrier is indicated by a vertical arrow.

include the channels listed in Table I, where T stands for target and P for projectile. The subindex in the case of the inclusion of the two-phonon states of the vibrational model indicates the order of the appearance of the specific spin value. The deformation parameters for the quadrupole (β_2) and octupole (β_3) deformations of the nuclear surface were taken from Refs. [47] and [48], respectively.

Comparing the data with the predictions of the one-dimensional barrier penetration model, we conclude that there are very strong enhancements of the experimental cross sections at sub-barrier energies. The enhancement is weaker in the case of the lighter ^{16}O projectile, because of its lower charge and, consequently, weaker coupling strength. One observes also that the predictions of our CC calculations are accurate at near-barrier energies for the four reactions. However, they underestimate the data at energies far below the barrier energy. The exception is the case of ^{16}O, for which the theoretical predictions are accurate for all energies. The inaccuracy of the theoretical predictions for the remaining three reactions indicates that other channels are playing important roles at energies well below the Coulomb barrier. The influence of these channels can be observed more clearly if one reduces the data, minimizing the influence of the rotational couplings. For this purpose, we use the procedure of the previous section, including all relevant rotational channels in set $\mathcal{A}$. These channels are the ones listed in Table I. The probable candidates for the space $\mathcal{B}$ are the real or virtual transfer channels.

Figure 4 shows the resulting renormalized experimental fusion functions $\bar{F}_{\rm exp}(x)$ for the four reactions. They are in very good agreement with the UFF for all reactions above $x \gtrsim -1$, which corresponds roughly to $E_{\rm c.m.} \gtrsim -4$ MeV. Below this value, the experimental fusion functions for the three heavier reactions exceed the UFF. Because transfer reactions are known to dominate the reaction cross section at very low energies (see, e.g., Fig. 5 of Ref. [49]), it is very likely that this discrepancy is because of the couplings to the transfer channels.

TABLE I. Coupling scheme used in the CC calculations for all reactions studied in this work.

System	Channels[a]
^{48}Ca + ^{154}Sm	2^+ 4^+ (T); 2^+ (P)
^{32}S + ^{154}Sm	2^+ 4^+ (T); 2_1^+ 0_2^+ 2_2^+ 4_1^+ (P)
^{28}Si + ^{154}Sm	2^+ 4^+ (T); 2^+ (P)
^{16}O + ^{154}Sm	2^+ 4^+ (T); 3^- (P)
^{58}Ni + ^{74}Ge	2_1^+ 2_2^+ 4_1^+ 0_2^+ (T); 2_1^+ 4_1^+ 2_2^+ 0_2^+ (P)
^{74}Ge + ^{74}Ge	2_1^+ 2_2^+ 4_1^+ 0_2^+ (T); 2_1^+ 2_2^+ 4_1^+ 0_2^+ (P)
^{132}Sn + ^{64}Ni	2_1^+ 2_2^+ 4_1^+ 3_1^- (T); 2_1^+ 3_1^- (P)

[a]T, target; P, projectile.

The fusion function for ^{16}O projectiles exhibits a different behavior. All experimental points are in good agreement with the UFF. Qualitatively, this result is consistent with the predictions of the neck formation model. The system size parameter of Ref. [6] for ^{16}O + ^{154}Sm is $\zeta = 18.6$ and the corresponding asymptotic shift is negligible (see Fig. 2 of Ref. [6]). Therefore, the bulk contribution of the transfer channels, represented by the neck formation degree of freedom, is very small.

B. Fusion in collisions of ^{58}Ni, ^{74}Ge + ^{74}Ge

We now investigate the fusion in the ^{58}Ni, ^{74}Ge + ^{74}Ge collisions. Data are from Refs. [50] and [51]. These reactions are particularly interesting because of the large deviations observed in systematic studies based on neck formation models [6,7]. They predict asymptotic shifts of $\Delta E_{\rm neck} \sim 7$ MeV, whereas the experimental shift is $\Delta E_{\rm exp} \sim 14$ MeV. This indicates that the average properties of the nuclear matter can only account for one-half of the observed values. The difference should then be attributed to the specific nuclear

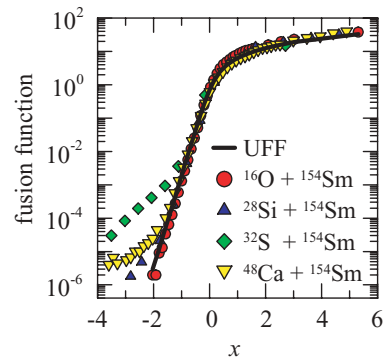

FIG. 4. (Color online) Experimental fusion cross sections in collisions of several projectiles with ^{154}Sm targets. The cross sections are reduced according to expressions (1) and (3) and the UFF is also shown (solid line).

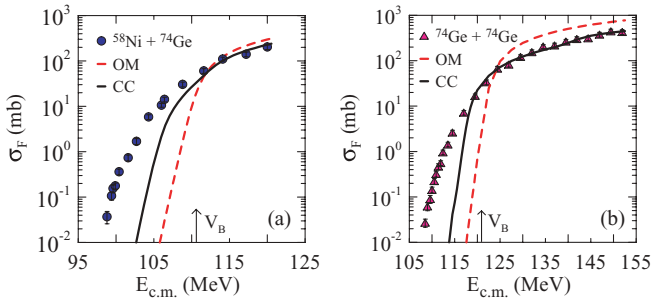

FIG. 5. (Color online) Experimental fusion cross sections for the reactions of (a) ^{58}Ni + ^{74}Ge and (b) ^{74}Ge + ^{74}Ge. The solid and dashed lines represent, respectively, the predictions of CC calculations including the channels of Table I and the predictions of the optical model (all couplings switched off).

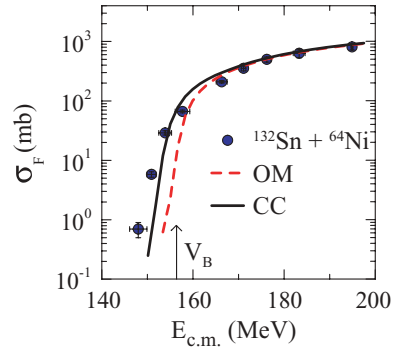

FIG. 7. (Color online) Comparison of the fusion cross-section data with OM and CC calculations for the reaction of ^{132}Sn + ^{64}Ni.

structure properties of these systems. The probable reason is that the ^{74}Ge nucleus is very soft with respect to deformations. Different studies lead to conflicting conclusions about its shape. Aguilera *et al.* [52] claim that it has a prolate deformation, whereas the CC analysis of Esbensen [53] of ^{74}Ge + ^{74}Ge fusion indicates that the data are more compatible with the vibrational coupling, with multiphonon excitation. The most likely situation is that the ground state of ^{74}Ge is an admixture of different shapes, which can easily be modified by the action of an external field. In this way, the formation of a neck between the projectile and the target is favored.

Figure 5 shows the experimental fusion cross sections for the ^{58}Ni, ^{74}Ge + ^{74}Ge reactions in comparison with the predictions of CC calculations (solid lines) and the results of the optical model (dashed lines). The deformation parameters were taken from Refs. [47] and [48]. One can see that the data are strongly enhanced with respect to the dashed lines. Although the CC calculations give good descriptions of the data at near-barrier energies, they underestimate the experimental cross sections at energies far below the barrier. The situation is analogous to that encountered in the previous subsection. This appears more clearly in Fig. 6, where the same cross sections are reduced and compared with the UFF. The probable reason for the discrepancies in this energy region is the influence of neck formation. The large deviations of the fusion functions with respect to the UFF are compatible with the above-mentioned discrepancy observed in the neck formation model.

C. Fusion in the neutron-rich ^{132}Sn with ^{64}Ni target

A similar investigation was performed for one reaction measured at Oak Ridge National Laboratory [39,40]. ^{132}Sn is a very neutron-rich radioactive projectile. The inelastic channels included in the coupling scheme are shown in Table I. The deformation parameters for the quadrupole (β_2) and octupole (β_3) deformations of the nuclear surface were taken from Refs. [54] and [55], respectively. The results are shown in Fig. 7, and the corresponding renormalized fusion function is shown in Fig. 8. One can observe that there is reasonable agreement between the fusion cross-section data and the theoretical predictions and between the renormalized fusion function and the UFF. However, some enhancement of the fusion cross section and the renormalized fusion function can be observed in relation to the calculation and the UFF, respectively. This effect, however, is not strong. Unfortunately, data are not available at lower energies, where deviations from the CC calculations and the UFF might show up.

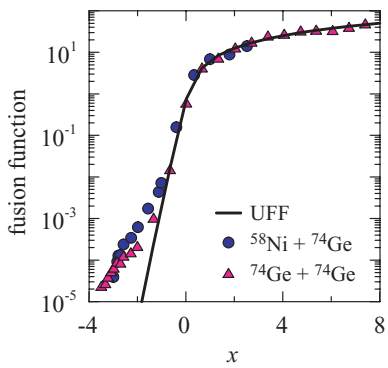

FIG. 6. (Color online) Reduced fusion cross sections of the reactions of Fig. 5, in comparison with the UFF.

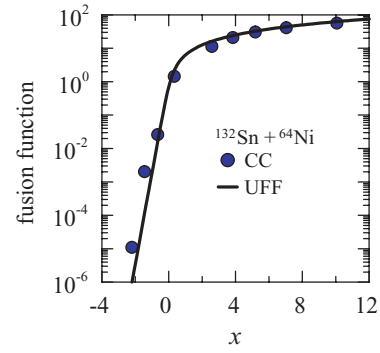

FIG. 8. (Color online) Comparison of the reduced fusion cross section for the reaction of ^{132}Sn + ^{64}Ni with the UFF. See text for details.

V. CONCLUSIONS

A recently proposed reduction method was used to investigate the influence of the transfer and neck formation in the fusion cross section. This study considers a few reactions where the fusion cross section is strongly influenced by couplings to inelastic channels. First we considered collisions of the highly deformed ^{154}Sm nucleus with several projectiles. We compared the reduced experimental data for these different reactions among themselves and with the universal fusion function. All reduced cross sections were close to the universal function in the barrier region and above it, indicating that couplings with rotational channels fully account for the couplings in this energy regime. However, at lower energies there are significant residual enhancements for the three heavier reactions, the exception being collision with the lighter ^{16}O projectile.

We also investigated the fusion cross sections for ^{58}Ni and ^{74}Ge + ^{74}Ge. In the reduction method, we included the main inelastic channels. The comparison of the reduced data with the universal function leads to similar conclusions: good agreement in the barrier region and residual enhancement well below the barrier. It is argued that this enhancement arises from very strong transfer couplings.

Finally, we investigated the fusion cross section for the radioactive neutron-rich ^{132}Sn projectile with ^{64}Ni target. One observes only a small deviation from the universal fusion function at the lowest energy, but no more data are available for the lower sub-barrier energy region, where the neck formation effect might show up.

In the future, it will be interesting to extend the present analysis for all the reactions where fusion cross-section data are available at energies well below the barrier to investigate the generality of the conclusions that were obtained for the few systems investigated.

We would like to mention that other reasons for the sub-barrier enhancements observed in the reactions cannot be ruled out. In studies with different approaches, such as proximity potentials, good results are obtained by changing the curvature and radius of the potential and by considering the Skyrme energy-density formalism, as already mentioned.

ACKNOWLEDGMENTS

This work was supported in part by the Fundacao de Amparo a Pesquisa do Estado do Rio de Janeiro (FAPERJ), Conselho Nacional de Desenvolvimento Cientifico e tecnologico (CNPq), and the Programa de Apoio a Nucleos de Excelencia (PRONEX). P.L. thanks the Instituto de Física da Universidade Federal do Rio de Janeiro for the hospitality and support during his visit to Rio.

[1] M. Beckerman, Rep. Prog. Phys. **51**, 1047 (1988).
[2] C. A. Bertulani, L. F. Canto, and M. S. Hussein, Phys. Rep. **226**, 281 (1993).
[3] A. B. Balanketin and N. Takigawa, Rev. Mod. Phys. **70**, 77 (1998).
[4] M. Dasgupta, D. J. Hinde, N. Rowley, and A. M. Stefanini, Annu. Rev. Nucl. Part. Sci. **48**, 401 (1998).
[5] L. F. Canto, P. R. S. Gomes, R. Donangelo, and M. S. Hussein, Phys. Rep. **424**, 1 (2006).
[6] C. E. Aguiar, V. C. Barbosa, L. F. Canto, and R. Donangelo, Phys. Lett. B **201**, 22 (1988).
[7] C. E. Aguiar, A. N. Aleixo, V. C. Barbosa, L. F. Canto, and R. Donangelo, Nucl. Phys. A **500**, 195 (1989).
[8] L. F. Canto, P. R. S. Gomes, J. Lubian, L. C. Chamon, and E. Crema, J. Phys. G **36**, 015109 (2009); Nucl. Phys. A **821**, 51 (2009).
[9] P. R. S. Gomes, J. Lubian, and L. F. Canto, Phys. Rev. C **79**, 027606 (2009).
[10] H. J. Krappe, J. R. Nix, and A. J. Sierk, Phys. Rev. C **20**, 992 (1979).
[11] J. Blocki, J. Randrup, W. J. Swiatecki, and C. F. Tsang, Ann. Phys. (NY) **105**, 427 (1977).
[12] P. R. Christensen and A. Winther, Phys. Lett. B **65**, 19 (1976).
[13] R. Bass, Phys. Rev. Lett. **39**, 265 (1977).
[14] K. Siwek-Wilczynska and J. Wilczynski, Phys. Lett. B **74**, 313 (1978).
[15] R. K. Puri, P. Chattopadhyay, and R. K. Gupta, Phys. Rev. C **43**, 315 (1991).
[16] R. K. Puri and R. K. Gupta, Phys. Rev. C **45**, 1837 (1992).
[17] R. K. Puri, M. K. Sharma, and R. K. Gupta, Eur. Phys. J. A **3**, 277 (1998).
[18] R. Arora *et al.*, Eur. Phys. J. A **8**, 103 (2000).
[19] R. K. Puri and N. K. Dhiman, Eur. Phys. J. A **23**, 429 (2005).
[20] H. Ngo and Ch. Ngo, Nucl. Phys. A **348**, 140 (1980).
[21] V. Yu Denisov and V. A. Nesterov, Phys. At. Nucl. **69**, 1472 (2006).
[22] M. A. Candido Ribeiro, L. C. Chamon, D. Pereira, M. S. Hussein, and D. Galetti, Phys. Rev. Lett. **78**, 3270 (1997).
[23] L. C. Chamon *et al.*, Phys. Rev. C **66**, 014610 (2002).
[24] G. R. Satchler and W. G. Love, Phys. Rep. **55**, 183 (1979).
[25] M. E. Brandan and G. R. Satchler, Phys. Rep. **285**, 143 (1997).
[26] C. P. Silva *et al.*, Nucl. Phys. A **679**, 287 (2001).
[27] J. J. S. Alves *et al.*, Nucl. Phys. A **748**, 59 (2005).
[28] L. R. Gasques, L. C. Chamon, P. R. S. Gomes, and J. Lubian, Nucl. Phys. A **764**, 135 (2006).
[29] D. Pereira, J. Lubian, J. R. B. Oliveira, D. P. Sousa, and L. C. Shamon, Phys. Lett. B **670**, 330 (2009).
[30] E. Crema, L. C. Chamon, and P. R. S. Gomes, Phys. Rev. C **72**, 034610 (2005).
[31] D. R. Otomar *et al.*, Phys. Rev. C **80**, 034614 (2009).
[32] E. Crema, P. R. S. Gomes, and L. C. Chamon, Phys. Rev. C **75**, 037601 (2007).
[33] P. R. S. Gomes *et al.*, J. Phys. G **31**, S1669 (2005).
[34] J. M. Figueira *et al.*, Phys. Rev. C **73**, 054603 (2006).
[35] J. M. Figueira *et al.*, Phys. Rev. C **75**, 017602 (2007).
[36] J. Lubian *et al.*, Nucl. Phys. A **791**, 24 (2007).
[37] P. R. S. Gomes, J. Lubian, I. Padrón, and R. M. Anjos, Phys. Rev. C **71**, 017601 (2005).
[38] C. Y. Wong, Phys. Rev. Lett. **31**, 766 (1973).
[39] J. F. Liang, D. Shapira, C. J. Gross, R. L. Varner, J. R. Beene, P. E. Mueller, and D. W. Stracener, Phys. Rev. C **78**, 047601 (2008).

[40] J. F. Liang *et al.*, Phys. Rev. C **75**, 054607 (2007).
[41] J. R. Leigh *et al.*, Phys. Rev. C **52**, 3151 (1995).
[42] S. Gil *et al.*, Phys. Rev. Lett. **65**, 3100 (1990).
[43] P. R. S. Gomes *et al.*, Phys. Rev. C **49**, 245 (1994).
[44] A. M. Stefanini *et al.*, Eur. Phys. J. A **23**, 473 (2005).
[45] G. N. Knyazheva *et al.*, Phys. Rev. C **75**, 064602 (2007).
[46] I. J. Thompson, Comp. Phys. Rep. **7**, 167 (1988).
[47] T. S. Raman, C. W. Nestor Jr., and P. Tikkanen, At. Data Nucl. Data Tables **78**, 1 (2001).
[48] T. Kibédi and R. H. Spear, At. Data Nucl. Data Tables **80**, 35 (2002).
[49] J. Wiggins, R. Brooks, M. Beckerman, S. B. Gazes, L. Grodzins, A. P. Smith, S. G. Steadman, Y. Xiao, and F. Videbaek, Phys. Rev. C **31**, 1315 (1985).
[50] M. Beckerman, M. Salomaa, A. Sperduto, J. D. Molitoris, and A. Di Rienzo, Phys. Rev. C **25**, 837 (1982).
[51] M. Beckerman, M. K. Salomaa, J. Wiggins, and R. Rohe, Phys. Rev. C **28**, 1963 (1983).
[52] E. F. Aguilera, J. J. Vega, J. J. Kolata, A. Morsad, R. G. Tighe, and X. J. Kong, Phys. Rev. C **41**, 910 (1990).
[53] H. Esbensen, Phys. Rev. C **72**, 054607 (2005).
[54] R. L. Varner *et al.*, Eur. Phys. J. A **25**, 391 (2005).
[55] B. Fogelberg *et al.*, Phys. Rev. Lett. **73**, 2413 (1994).